Shape model for the molecular interpretation of the flexoelectric effect

Alberta Ferrarini*
Dipartimento di Chimica Fisica, Università di Padova, 2 via Loredan, 35131 Padova, Italy
(Received 11 January 2001; published 26 July 2001)

A mean-field model for the flexoelectric polarization in nematics is presented, based on a continuous description of director deformations coupled to the molecular degrees of freedom via surface interactions. In such a framework, a consistent picture of the flexoelectric effect is obtained, including both dipolar and quadrupolar contributions, with a realistic account of the molecular characteristics of shape and charge distribution. The method is aimed at establishing a quantitative link between chemical structure and flexoelectric response. It provides numerical estimates of the effect and its temperature dependence and allows the recognition of the relevant molecular features for its emergence. Application to some representative systems, comprising mesogenic molecules and photoisomerizable dopants, is considered; it is shown that simple interpretative schemes can be misleading and a comparison with experimental data is reported.

DOI: 10.1103/PhysRevE.64.021710 PACS number(s): 61.30.−v

I. INTRODUCTION

The nematic phase has $D_{\infty h}$ symmetry, and as such it is incompatible with the presence of spontaneous electric polarization. However, in the presence of deformation breaking the up-down symmetry, a dipole moment can be developed. For symmetry reasons, of the three elementary deformations only the splay and bend ones can be coupled with polarization, according to the linear relationship

$$\mathbf{P}=e_s\mathbf{n}(\boldsymbol{\nabla}\cdot\mathbf{n})+e_b(\boldsymbol{\nabla}\times\mathbf{n})\times\mathbf{n}. \tag{1}$$

This behavior was predicted more than 30 years ago by Meyer [1], who, recognizing the analogy with the phenomenon occurring in crystals, called it piezoelectricity. Later on, the name *flexoelectricity* was adopted [2], the coefficients e_s and e_b being denoted as flexoelectric coefficients.

The microscopic origin of flexoelectricity was devised by Meyer in the simultaneous presence of shape and electrical polarity in molecules. The mechanism can be easily grasped by considering the exemplar cases of wedge- and crescent-shaped molecules, respectively, with longitudinal and transversal dipoles, as sketched in Fig. 1. In the presence of splay and bend distortions, respectively, the alignments parallel and antiparallel to the director are made inequivalent by short-range interactions, in such a way that the molecular orientations that fit to the molecular shape are favored. The same idea is at the basis of the works by Helfrich [3] and Petrov and Derzhanski [4], who, using phenomenological approaches, could estimate the flexoelectric coefficients for simple prototypical asymmetric bodies.

Actually, the presence of steric and electric polarity is not a necessary requirement for flexoelectricity, as was suggested by Prost and Marcerou [5], who envisaged a different mechanism in the gradient of the quadrupolar density. Thus, even in the case of nonpolar molecules characterized by nonpolar ordering with respect to the local director, spontaneous polarization can arise as a consequence of the phase inhomogeneity associated with director distortions.

General approaches that were based on different models for the intermolecular interactions, and were therefore able to take into account both kinds of mechanisms, were also presented: they go from the Onsager-like theory of Straley [6] to the molecular-field model formulated by Osipov [7], considering both attractive and repulsive short-range interactions, and the density-functional methods developed by Singh and Singh [8] and by Somoza and Tarazona [9]. More recently, also Monte Carlo simulations for nematic [10] and smectic [11] phases have been reported, whereby wedge-shaped molecules are modeled by combining Lennard-Jones and Gay-Berne potentials.

So, it can be stated that the general features of flexoelectricity are now understood, and estimates of the e_s and e_b coefficients for prototype objects with the idealized shapes of cones and bent rods, having dipole moments parallel and perpendicular to the axis of alignment, respectively, can be obtained. On the other hand, no predictions are provided by the available theories for the flexoelectric behavior of real molecules, and only rather vague considerations can be drawn from the magnitude and direction of the dipole moments and from the similarity between the structures and

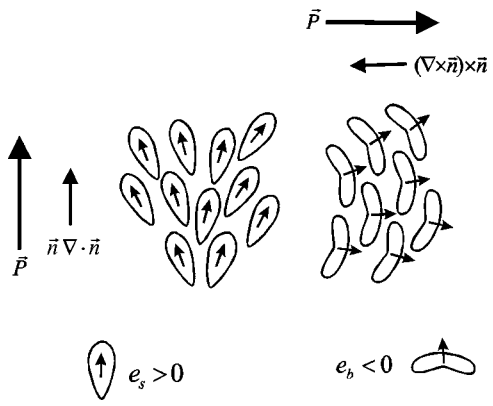

FIG. 1. Flexoelectric polarization according to the Meyer model (dipolar contribution).

*Email address: a.ferrarini@chfi.unipd.it

simple geometrical objects. Experimental measurements of flexoelectric coefficients, which have been performed with various methods, have also been of no great help, because of the ambiguity of the available results [12]. General agreement only exists about the order of magnitude of the flexoelectric coefficients, which range from a few to tens of pC/m. This makes them worth being taken into account in the analysis of electrostructural and electro-optic effects. Another point of interest in flexoelectricity derives from recently discovered linear electro-optic effects that exploit it [13]. All this points to the need for a better insight into the correlation between the molecular structure and the flexoelectric behavior.

The present work is motivated by the desire to make a contribution in this direction. So, a mean-field treatment has been set up, based on a continuum description of deformations in the mesophase, together with a phenomenological model for the coupling of the probe molecule and the director field, in terms of surface interactions between the molecule and the surrounding nematic. Such a mean field, which bears a formal analogy with the model for the anchoring free energy of macroscopic surfaces [2,14], is intended to account for the anisotropy of the short-range intermolecular interactions, which strongly depends on the molecular shape. The peculiar feature of the method is its ability to take into account the details of the chemical structure, entering through the molecular surface in the mean-field potential. The theory presented here is an extension to nematics with splay and bend deformations of an approach that has already been successfully used to predict the dependence on the molecular structure of the orientational order parameters in nematics [15–17], of the helical twisting power of chiral dopants [18–20], and of thermodynamic properties at the nematic-isotropic transition [21].

In the next section, the theory will be presented. Then the results obtained for some representative compounds will be reported, i.e., the well-studied mesogenic system N-(*p*-methoxybenzylidene)-*p'*-butylaniline (MBBA) [22–27] and a typical azodye, belonging to a class of molecules which have attracted some interest because the change of shape associated with the *cis-trans* photoisomerization is expected to have strong effects on the flexoelectric behavior [28–31].

II. THEORY

In the framework of the surface interaction model [15–17], it is assumed that each surface element *dS* of a molecule in the nematic phase tends to orient its normal **s** perpendicular to the local director **n**, according to the simple mean-field potential,

$$dU = k_B T \varepsilon P_2(\mathbf{n}\cdot\mathbf{s}), \tag{2}$$

where P_2 is the second Legendre polynomial and ε is a temperature-dependent parameter expressing the strength of the orienting interaction. The orientational behavior of the molecule is determined by the sum of contributions deriving from all surface elements,

$$U(\mathbf{\Omega}) = k_B T \varepsilon \int_S dS\ P_2(\mathbf{n}\cdot\mathbf{s}), \tag{3}$$

where the integral is performed over the molecular surface. The mean-field potential U depends on the molecular orientation, specified by the Euler angles $\mathbf{\Omega}=(\alpha,\beta,\gamma)$ describing the rotation from the laboratory to the molecular frame.

In deformed nematics, the director is a function of the space position. Thus, the mean field experienced by the surface element *dS* depends not only on its orientation, but also on its position. In order to make this dependence explicit, let us consider two points, identified by the vectors $\mathbf{R}_0$ and $\mathbf{R}=\mathbf{R}_0+\mathbf{r}$. If the distance r is much smaller than the length scale of the deformation, the position dependence of the nematic director **n** can be approximated as

$$\mathbf{n}(\mathbf{R}) \simeq \mathbf{n}(\mathbf{R}_0) + \sum_{I,J}\ \mathbf{e}_J(\nabla_I^{R_0} n_J) r_I, \tag{4}$$

where the labels *I,J,* denote the reference axes *(X,Y,Z)* of the laboratory frame, $\mathbf{e}_J$ is a unit vector parallel to the *J*th axis, and $\nabla_I^{R_0}$ indicates the I components of the gradient taken at $\mathbf{R}_0$. If Eq. (4) is substituted into Eq. (2), at first order in the displacement **r** the following expression is obtained for the mean field experienced by a surface element in **R**:

$$\begin{aligned} dU &= k_B T \varepsilon \left\{ P_2(\mathbf{n}\cdot\mathbf{s}) + 3(\mathbf{n}\cdot\mathbf{s}) \sum_{I,J}\ n_{J,I} r_I s_J \right\} \\ &= k_B T \varepsilon \left\{ P_2(\mathbf{n}\cdot\mathbf{s}) + 3 \sum_{I,J,K}\ n_K n_{J,I} r_I s_J s_K \right\}, \end{aligned} \tag{5}$$

where $\mathbf{n}=\mathbf{n}(\mathbf{R}_0)$ and $n_{J,I}=\nabla_I^{\mathbf{R}_0} n_J$. It is now convenient to consider a molecular frame; the mean field experienced by a molecule with the origin of this frame in $\mathbf{R}_0$ is obtained by integrating Eq. (5) over the whole molecular surface:

$$\begin{aligned} U(\mathbf{R}_0,\mathbf{\Omega}) = k_B T \varepsilon \Bigg\{ & \int_S dS\ P_2(\mathbf{n}\cdot\mathbf{s}) \\ & + 3 \sum_{I,J,K}\ n_K n_{J,I} \int_S dS\ r_I s_J s_K \Bigg\}, \end{aligned} \tag{6}$$

where **r** is the vector position of the surface element *dS* in the molecular frame.

Using this mean field, it is possible to calculate the electric polarization of deformed nematics, given the charge distribution $\rho(\mathbf{r}')$ of the constituent molecules. The polarization $\mathbf{P}(\mathbf{R}_0)$ can be expressed by a multipolar expansion [32]:

$$\begin{aligned} \mathbf{P}(\mathbf{R}_0) = N \Bigg\{ & \left\langle \int d\mathbf{r}'\, \rho(\mathbf{r}')\mathbf{r}' \right\rangle - (1/2)\nabla^{\mathbf{R}_0} \cdot \left\langle \int d\mathbf{r}'\, \rho(\mathbf{r}')\mathbf{r}' \right. \\ & \left. \otimes \mathbf{r}' \right\rangle + \cdots \Bigg\}, \end{aligned} \tag{7}$$

where N is the number density and the angular brackets denote orientational averages:

$$\langle \cdots \rangle = \int d\mathbf{\Omega}\ f(\mathbf{R}_0,\Omega)\cdots, \tag{8}$$

$f(\mathbf{R}_0,\mathbf{\Omega})$ being the orientational distribution function in $\mathbf{R}_0$, defined as

$$f(\mathbf{R}_0,\mathbf{\Omega}) = \frac{\exp[-U(\mathbf{R}_0,\mathbf{\Omega})/k_BT]}{\int d\mathbf{\Omega}\ \exp[-U(\mathbf{R}_0,\mathbf{\Omega})/k_BT]}. \tag{9}$$

This distribution function can be expanded about its value for undeformed nematics, and for small deformations the expansion can be truncated at the term linear in the deformation:

$$f(\mathbf{R}_0,\mathbf{\Omega}) \simeq f_0(\mathbf{\Omega})\left\{1 - 3\varepsilon \sum_{I,J,K} n_K n_{J,I} \int_S dS\ r_I s_J s_K\right\}, \tag{10}$$

where

$$f_0(\mathbf{\Omega}) = \frac{\exp[-U_0(\mathbf{\Omega})/k_BT]}{\int d\mathbf{\Omega}\ \exp[-U_0(\mathbf{\Omega})/k_BT]} \tag{11}$$

and

$$U_0(\mathbf{\Omega}) = k_BT\varepsilon \int_S dS\ P_2(\mathbf{n}\cdot\mathbf{s}) \tag{12}$$

are the distribution function and the mean field in the undeformed nematic phase. If the molecular charge distribution is approximated as a set of point charges $\rho(\mathbf{r}') = \Sigma_\alpha q_\alpha \delta(\mathbf{r}' - \mathbf{r}^\alpha)$ and only the first two terms of the multipolar expansion, corresponding, respectively, to the dipolar and the quadrupolar contribution, are retained, Eq. (7) can be rewritten as

$$\mathbf{P}(\mathbf{R}_0) \simeq N\left\{\sum_\alpha q_\alpha \langle \mathbf{r}^\alpha \rangle - (1/2)\sum_\alpha q_\alpha \nabla^{\mathbf{R}_0} \cdot \langle \mathbf{r}^\alpha \otimes \mathbf{r}^\alpha \rangle\right\}. \tag{13}$$

At first order in the deformation, we can write

$$\langle \mathbf{r}^\alpha \rangle \simeq -3\varepsilon \sum_{I,J,K} n_K n_{J,I} \int_S dS \langle \mathbf{r}^\alpha r_I s_J s_K \rangle_0, \tag{14}$$

where the zero apex indicates the average with respect to the undeformed distribution function Eq. (11), and the relation $\langle \mathbf{r}^\alpha \rangle_0 = \mathbf{0}$ has been used. Correspondingly, in the quadrupolar contribution of Eq. (13),

$$\nabla^{\mathbf{R}_0} \langle \mathbf{r}^\alpha \otimes \mathbf{r}^\alpha \rangle = \int d\mathbf{\Omega} [\nabla^{\mathbf{R}_0} f(\mathbf{\Omega})] \cdot \mathbf{r}^\alpha(\mathbf{\Omega}) \otimes \mathbf{r}^\alpha(\mathbf{\Omega}), \tag{15}$$

the gradient can be approximated as

$$\nabla_I^{\mathbf{R}_0} f(\mathbf{\Omega}) \simeq -3\varepsilon f_0(\mathbf{\Omega}) \sum_{J,K} n_K n_{J,I} \int_S dS \{s_J s_K - \langle s_J s_K \rangle_0\}. \tag{16}$$

The last term on the right-hand side of Eq. (16) vanishes, as can be seen by considering that (i) in a laboratory frame with an axis parallel to the undeformed director $\langle s_J s_K \rangle_0 = \langle s_J^2 \rangle_0 \delta_{JK}$, and (ii) the constant magnitude of the vector $\mathbf{n}$ implies $n_K n_{K,I} = 0$. Therefore, we can write

$$\nabla^{\mathbf{R}_0} \langle \mathbf{r}^\alpha \otimes \mathbf{r}^\alpha \rangle \simeq -3\varepsilon \sum_{I,J,K} n_K n_{J,I} \int_S dS \langle \mathbf{r}^\alpha r_I^\alpha s_J s_K \rangle_0. \tag{17}$$

By substituting Eqs. (14) and (17) into Eq. (13), the following expression for the flexoelectric polarization is obtained:

$$\mathbf{P} = -3N\varepsilon \sum_{I,J,K} n_K n_{J,I} \sum_\alpha q_\alpha \int_S dS \{\langle \mathbf{r}^\alpha r_I s_J s_K \rangle_0 - (1/2) \times \langle \mathbf{r}^\alpha r_I^\alpha s_J s_K \rangle_0\}. \tag{18}$$

The surface integrals on the right-hand side of this equation depend on the location of the origin of the molecular frame; this means that dipolar and quadrupolar contributions to the flexoelectric polarization cannot be unambiguously identified. However, it can be seen that the sum of the two contributions, and therefore the total polarization, is invariant with respect to a shift of the origin (see Appendix A).

To derive the explicit expression for the flexoelectric coefficients, it is convenient to take a laboratory frame with the Z axis parallel to the local director in $\mathbf{R}_0(Z \| \mathbf{n})$. In this frame, the splay and bend deformations can be expressed as

$$\begin{aligned} s &= s_Z = n_Z(n_{X,X} + n_{Y,Y}), \\ b_X &= n_Z n_{X,Z}, \\ b_Y &= n_Z n_{Y,Z}, \end{aligned} \tag{19}$$

which are, respectively, parallel and perpendicular to the director. Therefore, the components of the flexoelectric polarization can be expressed as

$$\begin{aligned} P_s &= P_Z = s_Z e_s, \\ P_b &= P_X + P_Y = (b_X + b_Y) e_b, \end{aligned} \tag{20}$$

with the flexoelectric coefficients e_s and e_b defined as

$$\begin{aligned} e_s &= -3N\varepsilon \sum_\alpha q_\alpha \int_S dS \{\langle r_Z^\alpha r_X s_X s_Z \rangle_0 - (1/2)\langle r_Z^\alpha r_X^\alpha s_X s_Z \rangle_0\} \\ &= -3N\varepsilon \int_S dS \{\langle \mu_Z r_X s_X s_Z \rangle_0 - \langle \Theta_{ZX} s_X s_Z \rangle_0\}, \end{aligned} \tag{21}$$

$$\begin{aligned} e_b &= -3N\varepsilon \sum_\alpha q_\alpha \int_S dS \{\langle r_X^\alpha r_Z s_X s_Z \rangle_0 - (1/2)\langle r_X^\alpha r_Z^\alpha s_X s_Z \rangle_0\} \\ &= -3N\varepsilon \int_S dS \{\langle \mu_X r_Z s_X s_Z \rangle_0 - \langle \Theta_{ZX} s_X s_Z \rangle_0\}, \end{aligned}$$

where $\boldsymbol{\mu}$ and $\boldsymbol{\Theta}$ are, respectively, the electric dipole and quadrupole tensors, with elements $\mu_I=\Sigma_\alpha q_\alpha r_I^\alpha$ and $\Theta_{IJ}=(1/2)\Sigma_\alpha q_\alpha r_I^\alpha r_J^\alpha$ [32].

It is customary to deal with the sum and difference of the flexoelectric coefficients:

$$\begin{aligned} e_s-e_b &= -3N\varepsilon\sum_\alpha q_\alpha\int_S dS\{\langle r_Z^\alpha r_X s_X s_Z\rangle_0-\langle r_X^\alpha r_Z s_X s_Z\rangle_0\} \\ &= -3N\varepsilon\int_S dS\{\langle \mu_Z r_X s_X s_Z\rangle_0-\langle \mu_X r_Z s_X s_Z\rangle_0\}, \end{aligned} \tag{22}$$

$$\begin{aligned} e_s+e_b &= -3N\varepsilon\sum_\alpha q_\alpha\int_S dS\{\langle r_Z^\alpha r_X s_X s_Z\rangle_0 \\ &\quad +\langle r_X^\alpha r_Z s_X s_Z\rangle_0-\langle r_X^\alpha r_Z^\alpha s_X s_Z\rangle_0\} \\ &= -3N\varepsilon\int_S dS\{\langle \mu_Z r_X s_X s_Z\rangle_0+\langle \mu_X r_Z s_X s_Z\rangle_0 \\ &\quad -2\langle \Theta_{XZ} s_X s_Z\rangle_0\}, \end{aligned}$$

where the former is only determined by the dipolar contribution, so it vanishes for nonpolar molecules, while the latter depends on both dipolar and quadrupolar terms. For the reasons seen above, both flexoelectric coefficients as well as their linear combinations are independent of the choice of the origin of the molecular frame.

Equations (21) and (22) show how the flexoelectric response is determined by the coupling of electrostatic and geometric properties of the molecules. The role of the molecular geometry appears even more clearly if the mean-field equation (6) is expressed in terms of irreducible tensor contributions, as shown in Appendix B. Such a reformulation of the problem is also useful to highlight the connection between the present approach and previous works [15,18], where the same basic assumptions adopted here to evaluate the flexoelectric effect were used to model the orientational order of molecules or the helical twisting power of chiral dopants in liquid crystals.

It appears from Eqs. (21) and (22) that, in contrast with simple theories, neither e_s+e_b nor e_s-e_b has a simple dependence on the orientational order parameters, since both of them depend on order parameters of various ranks. Actually things are even more complex, since the mesogenic molecules and, more generally, the molecules producing significant flexoelectric effects are usually fairly large and flexible. Therefore, the measured polarization cannot be simply associated with a single molecular structure, but it corresponds rather to the average over the conformational distribution. If, for the sake of simplicity, a discrete distribution over a finite number of conformers is considered, we can write

$$e_{s(b)}=\sum_n e_{s(b)}^n p^n, \tag{23}$$

where the apex indicates the nth conformer and p^n is its statistical weight:

$$p^n=\frac{\exp[-U_{\rm tors}^n/k_BT]\int d\boldsymbol{\Omega}\,\exp[-U_0^n(\boldsymbol{\Omega})/k_BT]}{\Sigma_n\exp[-U_{\rm tors}^n/k_BT]\int d\boldsymbol{\Omega}\,\exp[-U_0^n(\boldsymbol{\Omega})/k_BT]}, \tag{24}$$

$U_{\rm tors}^n$ and $U_0^n(\boldsymbol{\Omega})$ being, respectively, the torsional potential deriving from intramolecular interactions and the mean field experienced in undeformed nematics defined in Eq. (12), both evaluated for the nth conformer. The mean-field contribution has a magnitude of the order of some kJ mol^{-1}; it stabilizes the more elongated structures and has comparable values for conformers with similar shapes. Therefore, it can only produce small differences in the statistical weights p^n. On the contrary, large differences can arise from the torsional potential when strong intramolecular interactions occur in some of the conformers.

III. RESULTS AND DISCUSSION

As an application of the model, the flexoelectric coefficients of some typical systems have been evaluated. The molecular ingredients of the calculations are the surface and the charge distribution, which is described in terms of point charges located at the nuclear positions. In the case of systems with internal degrees of freedom, both have to be derived for each of the stable conformers. The use of accurate geometries is a major requirement in order to get reliable predictions since, as we shall see below, the flexoelectric behavior depends on the details of the molecular shape. In the present case, *ab initio* methods were used, as implemented in the package GAUSSIAN 98 [33]. In particular, geometry optimization was performed at the HF/6-31G* level, and then charges were obtained by applying to the optimized structures the Merz-Kollmann-Singh scheme [34], whereby charges are derived by fitting the electrostatic potential on the molecular surface. The rolling sphere algorithm, in the implementation by Sanner and co-workers [35], was used for the molecular surface. Therefore, this is defined as the surface drawn by a sphere of given radius rolling over the assembly of van der Waals beads centered at the atomic positions [36,16]. In the calculations, standard van der Waals radii were taken [37], and a rolling sphere radius equal to 3 Å was assumed, a sensible value to mimic the surface accessible to the solvent.

Scaled flexoelectric coefficients will be reported in the following, denoted as e_s^* and e_b^*, and defined as

$$e_{s(b)}^*=\frac{1}{N}e_{s(b)}. \tag{25}$$

They will be expressed in the units e Å^2, e being the electron charge; therefore, the relation between scaled and true flexoelectric coefficients, expressed in SI units, can be approximated as

$$e_{s(b)}\ \ ({\rm pC\ m^{-1}})\approx\frac{1000}{v\ \ ({\rm cm^3\ mol^{-1}})}e_{s(b)}^*(e\ {\rm Å}^2), \tag{26}$$

where v is the molar volume of the nematic phase.

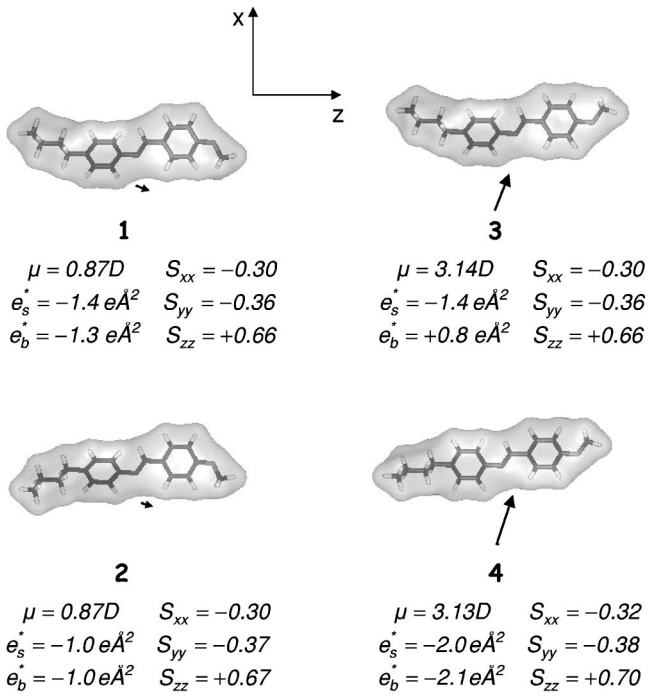

FIG. 2. Structure of the four conformers considered for MBBA, with the calculated dipole moments, orientational order parameters, and scaled flexoelectric coefficients.

The temperature dependence of the mean-field, Eq. (3), and then of the flexoelectric coefficients is contained in the orienting strength parameter ε. This has been simply modeled according to the Maier-Saupe theory [38]: the orienting strength of the nematic phase is only a function of the order parameter of the nematogenic molecules, $\overline{P_2^N}$, and of the nematic-isotropic transition temperature, T^{NI}. Thus, the expression for ε can be obtained from a comparison of the Maier-Saupe potential $U^{\mathrm{MS}}=-\varepsilon_0(\overline{P_2^N}T^{\mathrm{NI}})P_2(\cos\beta)$, where $\varepsilon_0=6.26\times10^{-23}$ J K^{-1}, with the surface interaction potential Eq. (3). Under the approximation of a nematic made of rigid uniaxial molecules, the latter can be rewritten as $U=-k_BT\varepsilon T_N^{20}P_2(\cos\beta)$, where T_N^{20} depends on the anisometry of the surface of the nematogenic molecules [15,16]; therefore, the expression

$$\varepsilon=\varepsilon_0\overline{P_2^N}/k_BT^*T_N^{20} \tag{27}$$

is obtained, with the reduced temperature $T^*=T/T^{\mathrm{NI}}$.

As a first example, we shall consider the nematogenic system MBBA, N-(*p*-methoxybenzylidene)-*p'*-butylaniline, whose flexoelectric coefficients were experimentally determined with various methods, leading to often contradictory results [22–27]. A nonplanar structure of the central core was obtained from geometry optimization, with a dihedral angle of about 40° between the planes containing the Ph-CH-N and the Ph-N groups, in agreement with theoretical and experimental findings. The four conformers shown in Fig. 2 were considered, differing in the values of the dihedral angles defining the orientations of the OCH_3 group (on either side of the attached phenyl ring) and of the *t*-butyl chain (above and below the linked phenyl ring) [39]. The *t*-butyl chain was taken in the all-*trans* conformation, since only minor effects were observed with other conformations. As can be seen from the figure, where also the surface is shown, none of the four conformers has a definite wedge or crescent shape, therefore simple considerations based on the behavior of prototypical objects would be completely inappropriate for MBBA. Figure 2 also reports the dipole moments of the four conformers, together with the flexoelectric coefficients and order parameters calculated with $\varepsilon=0.041$ Å^{-2}. The order parameters correspond to the principal axes of the ordering Saupe matrix, labeled in such a way that S_{yy} (<0) $<S_{xx}<S_{zz}$ (>0). It can be seen that the dipole moments of the two conformers 1-2 (with the O–CH_3 and CH–N bonds on the same side) are less than one-third of those calculated for the conformers 3-4 (having the O–CH_3 and CH–N bonds on opposite sides). Therefore, it is not surprising to see that the conformers 1 and 2 have similar flexoelectric coefficients, with a negligible dipolar contribution. On the contrary, the flexoelectric coefficients of the two other conformers are rather different, and show that the presence of a strong dipole moment is not sufficient to guarantee a significant dipolar contribution to the flexoelectric polarization. Actually, enhancement of the latter requires the matching of steric and electrostatic polarities. Analogies and differences between the various conformers also appear from Figs. 3(a) and 3(b), which show $e_s^*-e_b^*$ and $e_s^*+e_b^*$ as a function of the reduced temperature. The temperature dependence of the orienting strength ε is determined according to Eq. (27), with $T^{\mathrm{NI}}=320$ K and $T_N^{20}=75$ Å^2, values appropriate for MBBA. The flexoelectric coefficients of MBBA can be calculated from the scaled ones as $e_{s(b)}$ (pC m^{-1})$\approx 4e_{s(b)}^*$ (e Å^2). The comparison with experimental data is not obvious because the reported values are spread over a wide range [12]. However, there seems to be some agreement about the fact that e_s+e_b is negative, with values of the order of -15 to -30 pC/m, which decrease with a lowering of the reduced temperature [12]. The available data for e_s-e_b are scarcer; a positive value is reported, much smaller in magnitude than the sum e_s+e_b. The theoretical values to be compared with the experimental data should be obtained by averaging over all possible conformers, according to Eq. (23). Therefore, in our case we should consider, for each of the four isomers mentioned so far, all the possible conformers corresponding to one or more *gauche* bond in the alkyl chain. However, the introduction of *gauche* bonds does not change dramatically the molecular shape of MBBA, while it increases its torsional potential by at least 3 kJ mol^{-1} [39], thus lowering its statistical weight. Therefore, only the four conformers with all-*trans* chains will be considered, which have similar statistical weights, being characterized by the same torsional potential and comparable mean-field potentials. In the case of the sum e_s+e_b, all contributions are negative in sign and, with the exception of conformer 3, they are increasing functions of temperature; the average value, calculated according to Eq. (23) and displayed in Fig. 3(a), is also negative and ranges from -8 to -12 pC/m, in acceptable agreement with the experimental behavior. Less satisfactory seems to be the

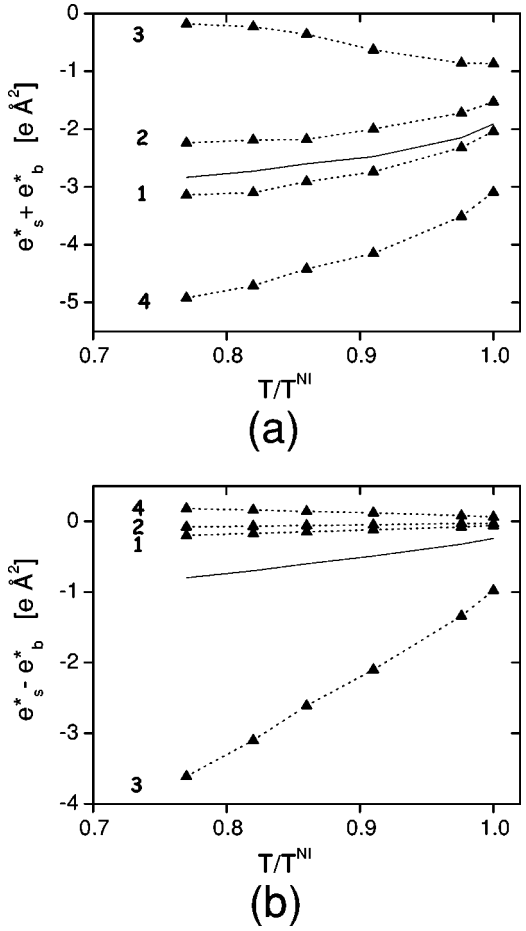

FIG. 3. Sum (a) and difference (b) of the scaled flexoelectric coefficients calculated with the four conformers of MBBA shown in Fig. 2. Solid lines are used for the average values.

comparison for the difference e_s-e_b, which is predicted to be negative ($e_s-e_b\approx-1$ to -3 pC/m). However, it should be considered that such a result is obtained by averaging contributions of opposite signs; this leads to a low value, significantly lower in absolute value than that of e_s+e_b, in agreement with experiment. Probably in cases of this sort the extension of the average to a larger number of conformers, in addition to a detailed knowledge of the molecular structures in the nematic phase, might be required to improve the quality of the predictions.

As a second example, the molecule of 4-hexyloxy-(4′-hexyl)azobenzene will be considered. Azodyes of this kind have recently been taken under consideration because the bent shape of the *cis* conformer obtained by photoisomerization seems to be appropriate to produce strong flexoelectric effects [28–31]. For 4-hexyloxy-(4′-hexyl)azobenzene, the ratio $(e_s-e_b)/K$, where K is the average elastic constant, was measured in 4 mol % mixtures in E7 (a commercial mixture of alkylcyanobiphenyls [40]), and negative values were observed both with and without uv irradiation, with a 40% increase in magnitude under *trans-cis* photoisomerization [30]. In this case, for a strict comparison with the experimental results the flexoelectric coefficients should be calculated by summing the contributions from all the species present in the mixture, i.e., the two forms of the azodye and the various components of the nematic solvent, each with all its relevant conformers. Moreover, a complete analysis of the experiment would require the prediction of the composition dependence of the NI transition temperature and of the elastic constants, and in particular their change under photoisomerization, again by taking into account the contributions from all the species. Such an analysis, beside being extremely costly, would go beyond our present purpose of simply providing estimates of the change in the flexoelectric coefficients associated with the change in the molecular geometry occurring in the *cis-trans* isomerization. Therefore, we have considered only the flexoelectric coefficients of the azodye, in its *cis* and *trans* forms, calculated under the approximation of infinite dilution. Thus the interaction strength parameter ε is determined according to Eq. (27), with $T^{\mathrm{NI}}=330$ K, the transition temperature of pure E7, and $T_N^{20}=78$ Å^2; with these choices, the dependence of ε on the reduced temperature is the same as that predicted for MBBA (see above). The contribution of 4-hexyloxy-(4′-hexyl)azobenzene to the flexoelectric coefficients of the E7-azodye mixture can be approximated as $e_{s(b)}$ (pC m^{-1})$\approx 4x e^*_{s(b)}$ (e Å^2), where x and $e^*_{s(b)}$ are the mole fraction and the flexoelectric coefficients of the azodye.

As in the case of MBBA, also for 4-hexyloxy-(4′-hexyl)azobenzene only the most stable conformers have been considered, with all-*trans* alkoxy and alkyl chains lying in all possible ways on the plane of the attached aromatic ring and perpendicular to it, respectively. The four and two conformers obtained, respectively, for the *cis* and the *trans* isomers are shown in Figs. 4 and 5, together with their dipole moments, the order parameters, and the scaled flexoelectric coefficients calculated with $\varepsilon=0.041$ Å^{-2}. For the *trans* isomers, the optimized geometry corresponds to a planar arrangement of the aromatic core, while in the case of the *cis* ones, distorted structures were obtained, with the dihedral angle C–N–N–C$\approx$5°, and phenyl rings rotated by $\approx$55° with respect to the N-N-C plane, in agreement with the reported experimental and theoretical values [41]. The *trans* isomers have a relatively small dipole moment and a rodlike shape. Accordingly, flexoelectric coefficients not particularly high, comparable with those obtained for MBBA, are predicted for them. Significantly higher flexoelectric coefficients are predicted for the *cis* isomers, which have larger dipole moments and shapes with definite polar asymmetries. In particular, as a consequence of their shapes, the conformers 1 and, to a lesser extent, 4 have a propensity to align their dipoles to the director (wedgelike behavior). On the contrary, a crescentlike behavior is predicted for the conformers 2 and 3, which are elongated in the direction perpendicular to the dipole, and are then expected to preferentially orient the dipole normal to the director. Correspondingly, large e_s^* and e_b^* values are predicted, respectively, for the 1,4 conformers and for the 2,3 ones. In comparing *cis* and *trans* isomers, it can also be noted that the latter have much higher order parameters. This is a consequence of their elongated shape, which makes them fit very well into the nematic phase. Figure 6(a) shows the temperature dependence of the sum $e_s^*+e_b^*$: relatively small

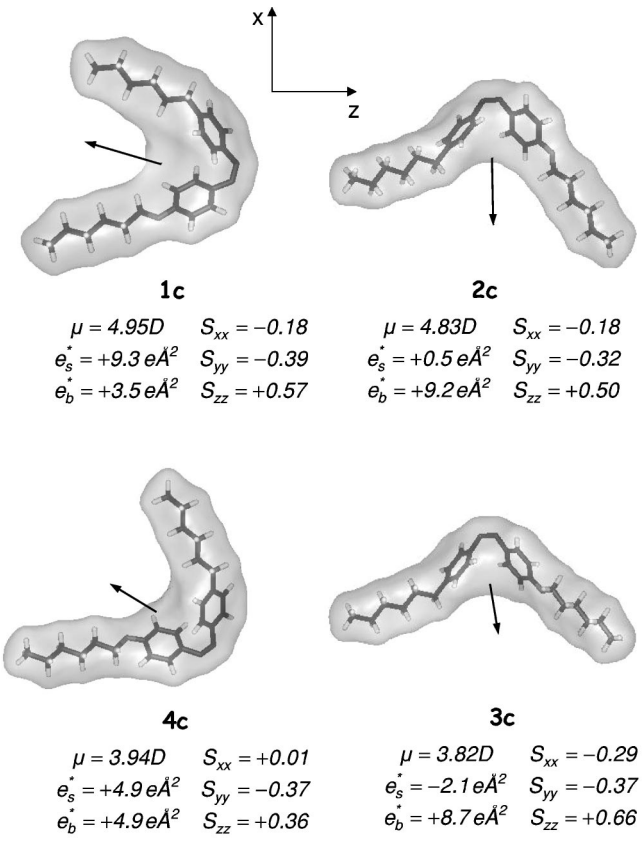

FIG. 4. Structure of the four *cis* conformers considered for 4-hexyloxy-(4′-hexyl)azobenzene, with the calculated dipole moments, orientational order parameters, and scaled flexoelectric coefficients.

values, comparable with those obtained for MBBA, and negative in sign, are predicted for the *trans* isomers, while high and positive values are obtained for the *cis* structures. Considering now the difference $e_s^* - e_b^*$, whose temperature dependence is shown in Fig. 6(b), we see that it is small for the *trans* conformers, as a consequence of the small shape

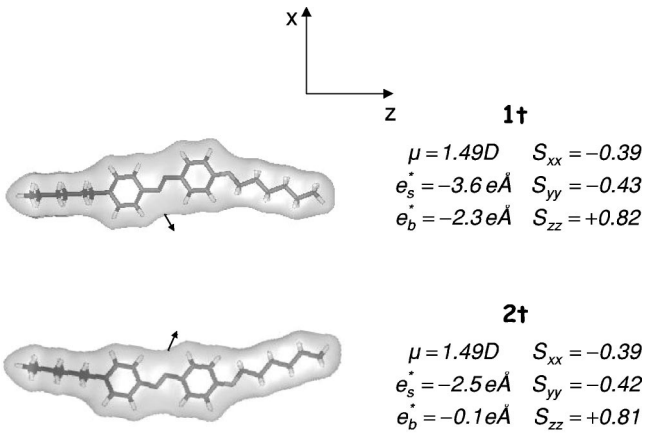

FIG. 5. Structure of the two *trans* conformers considered for 4-hexyloxy-(4′-hexyl)azobenzene, with the calculated dipole moments, orientational order parameters, and scaled flexoelectric coefficients.

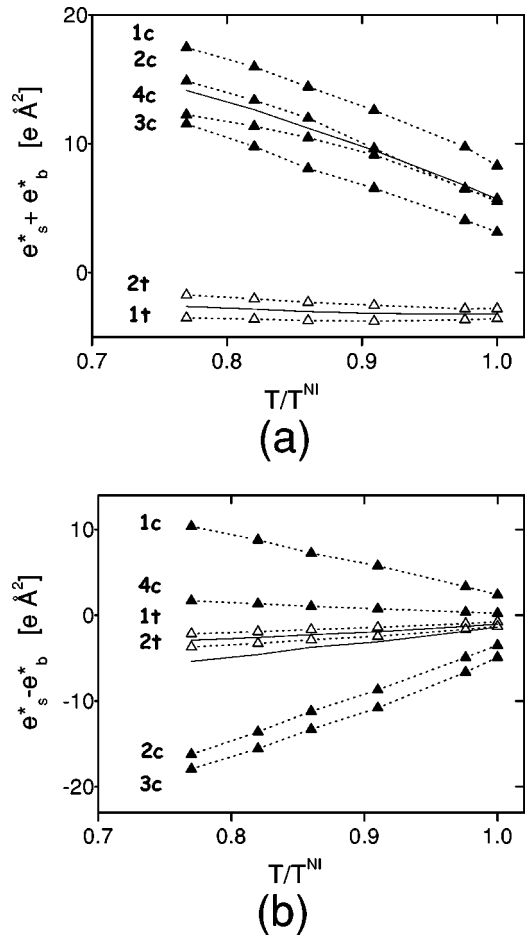

FIG. 6. Sum (a) and difference (b) of the scaled flexoelectric coefficients calculated with the six conformers of 4-hexyloxy-(4′-hexyl)azobenzene shown in Figs. 4 and 5. Solid lines indicate the average values for *cis* and *trans* isomers.

and charge polarity. Much higher values are predicted for the *cis* conformers, positive and negative for the crescent- and the wedge-shaped molecules, respectively. The average *trans* and *cis* values, calculated according to Eq. (23), are both negative and fall in the ranges -1 to -3 pC/m (*trans*) and -1.5 to -6 pC/m (*cis*). A direct comparison with the data reported in Ref. [30], that is, the ratio $(e_s - e_b)/K$ measured for pure E7 and for E7 doped with the azodye before and after uv irradiation, cannot be made because the experimental results depend not only on the different flexoelectric response of the two isomers, but also on the isomerization yield and on the change of ordering and elastic constants associated with the photoisomerization process. The former might be only a minor problem since the conversion is likely to be almost complete, but there is much more uncertainty about the latter contributions. At most, we can guess that they should have opposite effects on the ratio $(e_s - e_b)/K$, since the *trans*→*cis* isomerization is accompanied by a decrease of the NI transition temperature [42], and thus a decrease of ordering and probably a decrease of the average elastic constant. Thus, considering that the comparison between theoretical results and the experimental data reported in Ref. [30] cannot go beyond the qualitative level, we can

conclude that a general agreement is found: the measured and predicted difference of flexoelectric coefficients is negative in sign for both the *trans* and the *cis* isomers, and significantly larger in magnitude for the latter. Finally, it is worth mentioning that the flexoelectric coefficients reported here for 4-hexyloxy-(4′-hexyl)azobenzene strongly depend on the chemical structure, and cannot be immediately generalized to any azodye. Indeed, significant effects on the flexoelectric behavior are predicted not only for a shortening of the flexible chains, in which case a weaker flexoelectric response is estimated, but also for a small chemical modification such as the insertion of an oxygen atom between the phenyl ring and the alkyl chain. This agrees with the indications derived from experiments, from which a nontrivial dependence on the details of the chemical structure can be inferred [31].

IV. CONCLUSIONS

In this work, a molecular theory for the flexoelectric effect in nematics has been presented that, adopting a simple mean-field picture, is intended to take into account in a realistic way the relevant molecular features. The model has to be seen in the more general framework of a theoretical approach aimed at correlating molecular structure with order and macroscopic properties of mesophases, which has already been shown to provide reliable estimates of orientational order parameters and transition properties of nematic phases, as well as the helical pitch of twisted nematics [15–20].

As an application of the model, the flexoelectric coefficients of some typical systems have been calculated as a function of the molecular structure, which enters through the molecular surface and charge distribution, by explicitly considering, when required, the presence of several conformers. In this way, a detailed analysis of the flexoelectric behavior and its dependence on the molecular properties can be performed. Comparison with experimental data, when available, shows that the magnitude of the effects is correctly predicted. Therefore, it is hoped that the approach presented here can be of some help to shed light on the molecular origin of the flexoelectric response and, therefore, to optimize materials for its exploitation.

ACKNOWLEDGMENTS

This work was supported by MURST PRIN ex 40%, EC (TMR Contract No. FMRX CT97 0121) and CNR, through its Centro Studi sugli Stati Molecolari. The author wishes to thank Professor G. J. Moro for valuable discussions.

APPENDIX A

In order to demonstrate that the total polarization is invariant for a shift of the origin of the molecular frame, let us take the translation $O^0 \rightarrow O$, so that $\mathbf{r}^\alpha = \mathbf{r}^{\alpha 0} + \Delta\mathbf{r}$ and $\mathbf{r} = \mathbf{r}^0 + \Delta\mathbf{r}$; then we can write

$$\sum_\alpha q_\alpha \langle r_M^\alpha r_I s_J s_K \rangle_0 = \sum_\alpha q_\alpha \langle r_M^{\alpha 0} r_I^0 s_J s_K \rangle_0 + \sum_\alpha q_\alpha \langle r_M^{\alpha 0} \Delta r_I s_J s_K \rangle_0, \quad \text{(A1)}$$

$$\sum_\alpha q_\alpha \langle r_M^\alpha r_I^\alpha s_J s_K \rangle_0 = \sum_\alpha q_\alpha \langle r_M^{\alpha 0} r_I^{\alpha 0} s_J s_K \rangle_0 + (1/2) \sum_\alpha q_\alpha \langle \Delta r_M r_I^{\alpha 0} s_J s_K \rangle_0 + (1/2) \sum_\alpha q_\alpha \langle r_M^{\alpha 0} \Delta r_I s_J s_K \rangle_0, \quad \text{(A2)}$$

which have been derived by exploiting the relation $\Sigma_\alpha q_\alpha = 0$, which holds for neutral molecules. By using the relation between the components in the laboratory frame $\{X,Y,Z\}$ and those in a molecular frame $\{x,y,z\}$ coincident with the principal frame of the tensor $\mathbf{s}\otimes\mathbf{s}$, $v_I = \Sigma_i e_{iI}(\mathbf{\Omega}) v_i$, where e_{iI} is the component of the Ith laboratory axis along the ith molecular axis, the following equalities result:

$$\langle \Delta r_M r_I^{\alpha 0} s_J s_K \rangle_0 = \sum_{m,i,j} r_m^{\alpha 0} \Delta r_i s_j s_j \langle e_{mM} e_{iI} e_{jJ} e_{jK} \rangle_0 = \sum_{m,j} r_m^{\alpha 0} \Delta r_m s_j s_j \langle e_{mM} e_{mI} e_{jJ} e_{jK} \rangle_0 = \langle \Delta r_I r_M^{\alpha 0} s_J s_K \rangle_0, \quad \text{(A3)}$$

where the local axial symmetry of the phase has been taken into account. Therefore, Eq. (A2) can be rewritten as

$$\sum_\alpha q_\alpha \langle r_M^\alpha r_I^\alpha s_J s_K \rangle_0 = \sum_\alpha q_\alpha \langle r_M^{\alpha 0} r_I^{\alpha 0} s_J s_K \rangle_0 + \sum_\alpha q_\alpha \langle r_M^{\alpha 0} \Delta r_I s_J s_K \rangle_0, \quad \text{(A4)}$$

from which it follows that the difference between the two contributions Eqs. (A1) and (A2) is invariant for a shift of the origin of the molecular frame.

APPENDIX B

The integrand in the second term on the right-hand side of Eq. (6) is the contraction of the third-rank tensors $\nabla\otimes\mathbf{n}\otimes\mathbf{n}$ and $\mathbf{r}\otimes\mathbf{s}\otimes\mathbf{s}$, and it can be expressed as a linear combination of the invariants obtained by combining the irreducible parts of the two tensors. The reformulation in terms of irreducible tensors helps to make clear the connection of the present result with previous works based on the same assumption of surface interactions [15,18].

The third-rank tensor $\mathbf{a}\otimes\mathbf{b}\otimes\mathbf{c}$ can be decomposed in one zero-rank, three first-rank, two second-rank, and one third-rank irreducible tensor. The form of the resulting irreducible tensors depends on the vector coupling scheme. The expres-

TABLE I. Irreducible tensors obtained from the third-rank tensor $\mathbf{a}\otimes\mathbf{b}\otimes\mathbf{c}$.

λ	L	${}_\lambda T^{(L)}$
1	0	$-(i/\sqrt{6})\mathbf{a}\cdot(\mathbf{b}\times\mathbf{c})$
0	1	$-(1/\sqrt{3})\mathbf{a}(\mathbf{b}\cdot\mathbf{c})$
1	1	$(1/2)[(\mathbf{a}\cdot\mathbf{b})\mathbf{c}-(\mathbf{a}\cdot\mathbf{c})\mathbf{b}]$
2	1	$\sqrt{3/5}[(1/3)\mathbf{a}(\mathbf{b}\cdot\mathbf{c})-(1/2)(\mathbf{a}\cdot\mathbf{c})\mathbf{b}-(1/2)(\mathbf{a}\cdot\mathbf{b})\mathbf{c}]$
1	2	$(\imath/2\sqrt{2})\{(\mathbf{b}\times\mathbf{c})\otimes\mathbf{a}+\mathbf{a}\otimes(\mathbf{b}\times\mathbf{c})-(2/3)[\mathbf{a}\cdot(\mathbf{b}\times\mathbf{c})]\mathbf{I}_2\}$
2	2	$(\imath/2\sqrt{6})[\mathbf{b}\otimes(\mathbf{c}\times\mathbf{a})+(\mathbf{c}\times\mathbf{a})\otimes\mathbf{b}-\mathbf{c}\otimes(\mathbf{a}\times\mathbf{b})-(\mathbf{a}\times\mathbf{b})\otimes\mathbf{c}]$
2	3	$\mathcal{S}\{\mathbf{a}\otimes\mathbf{b}\otimes\mathbf{c}\}-(1/5)\mathcal{S}\{[(\mathbf{a}\cdot\mathbf{b})\mathbf{c}+(\mathbf{a}\cdot\mathbf{c})\mathbf{b}+(\mathbf{c}\cdot\mathbf{b})\mathbf{a}]\otimes\mathbf{I}_2\}$

sions obtained by first coupling **b** and **c** and then **a** are reported in Table I. The following notation is used: n vertical dots indicate contraction with respect to n indeces, $\times$ and $\otimes$ refer to vector and tensor products, respectively, $\mathbf{I}_2$ is the unit tensor of second rank, with $I_{i,j}=\delta_{i,j}$, and $\mathcal{S}\{\cdots\}$ denotes the symmetrized form of a tensor, $\mathcal{S}\{\mathbf{T}\}_{ijk}=(1/6)(T_{ijk}+T_{ikj}+T_{kij}+T_{kji}+T_{jki}+T_{jik})$. Finally, the symbol ${}_\lambda T^{(L)}$ is used for the irreducible tensor of rank L obtained by coupling a first-rank tensor with an irreducible tensor of rank λ deriving from the coupling of two first-rank tensors. The contraction of the two third-rank Cartesian tensors

$$\mathcal{I}=\mathbf{a}\otimes\mathbf{b}\otimes\mathbf{c}:\mathbf{d}\otimes\mathbf{e}\otimes\mathbf{f}=\sum_{I,K,J} a_I b_J c_K d_I e_J f_K \tag{B1}$$

can be rewritten in terms of its irreducible components

$$\mathcal{I}=\sum_{\lambda L} {}_\lambda(\mathbf{a}\otimes\mathbf{b}\otimes c)^{(L)}\vdots{}_\lambda(\mathbf{d}\otimes\mathbf{e}\otimes\mathbf{f})^{(L)}$$
$$=\sum_{\lambda=0}^{2}\ \sum_{L=|\lambda-1|}^{\lambda+1}\ \sum_{I} {}_\lambda(\mathbf{a}\otimes\mathbf{b}\otimes\mathbf{c})_I^{(L)}*{}_\lambda(\mathbf{d}\otimes\mathbf{e}\otimes\mathbf{f})_I^{(L)}. \tag{B2}$$

When the expressions for the irreducible tensors (Tables II and III) are used and the origin O of the molecular frame is set in the point defined by the relation

$$\int_S dS\ \mathbf{r}=\mathbf{0}, \tag{B3}$$

TABLE II. Irreducible tensors obtained from the third-rank tensor $\mathbf{r}\otimes\mathbf{s}\otimes\mathbf{s}$.

λ	L	${}_\lambda T^{(L)}$
1	0	0
0	1	$-(1/\sqrt{3})\mathbf{r}$
1	1	0
2	1	$\sqrt{3/5}[(1/3)\mathbf{r}-(\mathbf{s}\cdot\mathbf{r})\mathbf{s}]$
1	2	0
2	2	$(\imath/\sqrt{6})[\mathbf{s}\otimes(\mathbf{s}\times\mathbf{r})+(\mathbf{s}\times\mathbf{r})\otimes\mathbf{s}]$
2	3	$\mathcal{S}\{\mathbf{r}\otimes\mathbf{s}\otimes\mathbf{s}\}-(1/5)\mathcal{S}\{[\mathbf{r}+2(\mathbf{r}\cdot\mathbf{s})\mathbf{s}]\otimes\mathbf{I}_2\}$

TABLE III. Irreducible tensors obtained from the third-rank tensor $\nabla\otimes\mathbf{n}\otimes\mathbf{n}$.

λ	L	${}_\lambda T^{(L)}$
1	0	0
0	1	$-(1/\sqrt{3})(\nabla\otimes\mathbf{n})\cdot\mathbf{n}$
1	1	$(1/2)[-\mathbf{n}\cdot(\nabla\otimes\mathbf{n})+(\nabla\cdot\mathbf{n})\mathbf{n}]$
2	1	$\sqrt{3/5}[(1/3)(\nabla\otimes\mathbf{n})\cdot\mathbf{n}-(1/2)\mathbf{n}\cdot(\nabla\otimes\mathbf{n})-(1/2)(\nabla\cdot\mathbf{n})\mathbf{n}]$
1	2	
2	2	$(\imath/2\sqrt{6})\{\mathbf{n}\times\nabla\otimes\mathbf{n}+(\mathbf{n}\times\nabla\otimes\mathbf{n})^{\mathrm{Tr}}-\mathbf{n}\otimes(\nabla\times\mathbf{n})-(\nabla\times\mathbf{n})\otimes\mathbf{n}\}$
2	3	$\mathcal{S}\{\nabla\otimes\mathbf{n}\otimes\mathbf{n}\}-(1/5)\mathcal{S}\{[\mathbf{n}\cdot(\nabla\otimes\mathbf{n})+(\nabla\cdot\mathbf{n})\mathbf{n}+(\nabla\otimes\mathbf{n})\cdot\mathbf{n}]\otimes\mathbf{I}_2\}$

Eq. (6) can be rewritten as

$$U(\mathbf{R}_0,\boldsymbol{\Omega})=k_BT\varepsilon\Bigg\{(3/2)\mathbf{n}\cdot\int_S dS[\mathbf{s}\otimes\mathbf{s}-\tfrac{1}{3}\mathbf{I}_2]\cdot\mathbf{n}+(9/10)$$
$$\times\{(\nabla\cdot\mathbf{n})\mathbf{n}+[(\nabla\times\mathbf{n})\times\mathbf{n}]\}\cdot\int_S dS\ \mathbf{s}(\mathbf{s}\cdot\mathbf{r})$$
$$+(1/2)\{(\mathbf{n}\times\nabla)+(\nabla\times\mathbf{n})\}\cdot\int_S dS[\mathbf{s}\otimes(\mathbf{s}\times\mathbf{r})$$
$$+(\mathbf{s}\times\mathbf{r})\otimes\mathbf{s}]\cdot\mathbf{n}+3(\mathcal{S}\{\nabla\otimes\mathbf{n}\otimes\mathbf{n}\}$$
$$-(1/5)\mathcal{S}\{[\mathbf{n}\cdot(\nabla\otimes\mathbf{n})+(\nabla\cdot\mathbf{n})\mathbf{n}+(\nabla\otimes\mathbf{n})\cdot\mathbf{n}]$$
$$\otimes\mathbf{I}_2\})\vdots(\mathcal{S}\{\mathbf{r}\otimes\mathbf{s}\otimes\mathbf{s}\}-(1/5)\mathcal{S}\{[\mathbf{r}+2(\mathbf{r}\cdot\mathbf{s})\mathbf{s}]$$
$$\otimes\mathbf{I}_2\})\Bigg\}. \tag{B4}$$

According to previous work, we shall define the second-rank surface tensor **T**, accounting for the shape anisometry of the molecular surface [15]:

$$\mathbf{T}=-\frac{1}{\sqrt{6}}\int_S dS[3\mathbf{s}\otimes\mathbf{s}-\mathbf{I}_2], \tag{B5}$$

and the second-rank chirality pseudotensor **Q**, which describes the helicity of the molecular surface [18]:

$$\mathbf{Q}=\sqrt{\tfrac{3}{8}}\int_S dS[\mathbf{s}\otimes(\mathbf{s}\times\mathbf{r})+(\mathbf{s}\times\mathbf{r})\otimes\mathbf{s}]. \tag{B6}$$

Here we shall introduce the first-rank tensor **II**:

$$\mathbf{II}=\tfrac{9}{10}\int_S dS\ \mathbf{s}(\mathbf{s}\cdot\mathbf{r}), \tag{B7}$$

which will be denoted as a polarity tensor since it provides a measure of the polarity of the molecular surface, and the third-rank tensor $\boldsymbol{\Xi}$:

$$\Xi = \int_S dS(\mathcal{S}\{\mathbf{r}\otimes\mathbf{s}\otimes\mathbf{s}\} - (1/5)\mathcal{S}\{[\mathbf{r}+2(\mathbf{r}\cdot\mathbf{s})\mathbf{s}]\otimes\mathbf{I}_2\}). \tag{B8}$$

Then, Eq. (B4) can be rewritten as

$$\begin{aligned} U(\mathbf{R}_0,\mathbf{\Omega}) = k_B T\varepsilon\{&-\sqrt{\tfrac{3}{2}}\mathbf{n}\cdot\mathbf{T}\cdot\mathbf{n} + \{(\nabla\cdot\mathbf{n})\mathbf{n} + [(\nabla\times\mathbf{n}) \\ &\times\mathbf{n}]\}\cdot\mathbf{II} + \sqrt{\tfrac{2}{3}}\{(\mathbf{n}\times\nabla) - (\nabla\times\mathbf{n})\}\cdot\mathbf{Q}\cdot\mathbf{n} \\ &+ 3[\mathcal{S}\{\nabla\otimes\mathbf{n}\otimes\mathbf{n}\} - (1/5)\mathcal{S}\{[\mathbf{n}\cdot(\nabla\otimes\mathbf{n}) + (\nabla\cdot\mathbf{n})\mathbf{n} \\ &+ (\nabla\otimes\mathbf{n})\cdot\mathbf{n}]\otimes\mathbf{I}_2\}]\vdots\Xi\}. \end{aligned} \tag{B9}$$

The position and orientation dependence of the mean field is implicit in that of the director $\mathbf{n}$ and the surface integrals, respectively. In the case of undeformed nematics $\nabla\times\mathbf{n}=\mathbf{0}$ and $\nabla\cdot\mathbf{n}=\mathbf{0}$, so that only the first term survives; the mean-field potential has the ''surface tensor'' form, used to predict the orientational order in nematic phases [15,21]. For twisted nematics phases, characterized by $\nabla\cdot\mathbf{n}=0$ and $(\nabla\times\mathbf{n}) = -q\mathbf{n}$, where p is the pitch and $q=2\pi/p$ is the wave vector, the expression adopted in the model for the helical twisting power of chiral dopants is recovered [18].

By introducing the irreducible tensors defined so far into Eqs. (21), the expressions for the flexoelectric coefficients can be rewritten as

$$\begin{aligned} e_s = -3N\varepsilon\{&\langle\mu_Z\Pi_Z\rangle_0 + \tfrac{1}{5}[\langle\mu_Z\Xi_{ZZZ}\rangle_0 - 3\langle\mu_Z\Xi_{XXZ}\rangle_0] \\ &+ \sqrt{\tfrac{2}{3}}\langle\Theta_{ZX}T_{XZ}\rangle_0\}, \end{aligned} \tag{B10}$$

$$\begin{aligned} e_b = -3N\varepsilon\{&\langle\mu_X\Pi_X\rangle_0 + \sqrt{\tfrac{2}{3}}\langle\mu_X Q_{YZ}\rangle_0 + \tfrac{1}{5}[\langle\mu_X\Xi_{XXX}\rangle_0 \\ &+ \langle\mu_X\Xi_{XYY}\rangle_0 - 4\langle\mu_X\Xi_{ZZX}\rangle_0] + \sqrt{\tfrac{2}{3}}\langle\Theta_{ZX}T_{XZ}\rangle_0\}. \end{aligned}$$

[1] R. B. Meyer, Phys. Rev. Lett. **22**, 319 (1969).
[2] P. G. de Gennes and J. Prost, *The Physics of Liquid Crystals* (Clarendon, Oxford, 1993).
[3] W. Helfrich, Z. Naturforsch. C **26c**, 833 (1971).
[4] A. I. Derzhanski and A. G. Petrov, Phys. Lett. **36A**, 483 (1971).
[5] J. Prost and J. P. Marcerou, J. Phys. (France) **38**, 315 (1977).
[6] J. P. Straley, Phys. Rev. A **14**, 1835 (1976).
[7] M. A. Osipov, Zh. Eksp. Teor. Fiz. **85**, 2011 (1983) [Sov. Phys. JETP **58**, 1167 (1983)].
[8] Y. Singh and U. P. Singh, Phys. Rev. A **39**, 4254 (1989).
[9] A. M. Somoza and P. Tarazona, Mol. Phys. **72**, 911 (1991).
[10] J. Stelzer, R. Berardi, and C. Zannoni, Chem. Phys. Lett. **299**, 9 (1999).
[11] J. L. Billeter and R. A. Pelcovits, Liq. Cryst. **27**, 1151 (2000).
[12] A. G. Petrov, in *Physical Properties of Liquid Crystals, EMIS Datareview Series 25*, edited by D. A. Dunmur, A. Fukuda, and G. R. Luckhurst (IEE, London, 2001), and references therein.
[13] J.S. Patel and R.B. Meyer, Phys. Rev. Lett. **58**, 1538 (1987); P. Rudquist, M. Buiyvidas, L. Komitov, and S. T. Lagerwall, J. Appl. Phys. **76**, 7778 (1994).
[14] A. Rapini and M. Papoular, J. Phys. (Paris), Colloq. **30**, C4-54 (1969).
[15] A. Ferrarini, G. J. Moro, P. L. Nordio, and G. R. Luckhurst, Mol. Phys. **77**, 1 (1992).
[16] A. Ferrarini, F. Janssen, G. J. Moro, and P. L. Nordio, Liq. Cryst. **26**, 201 (1999).
[17] A. Ferrarini, G. J. Moro, and P. L. Nordio, in *Physical Properties of Liquid Crystals, EMIS Datareview Series 25* (Ref. [12]).
[18] A. Ferrarini, G. J. Moro, and P. L. Nordio, Phys. Rev. E **53**, 681 (1996).
[19] A. Ferrarini, P. L. Nordio, P. V. Shibaev, and V. P. Shibaev, Liq. Cryst. **24**, 219 (1998).
[20] A. Ferrarini, G. Gottarelli, P. L. Nordio, and G. P. Spada, J. Chem. Soc., Perkin Trans. 2 **1999**, 411 (1999).
[21] A. Ferrarini, G. R. Luckhurst, P. L. Nordio, and S. J. Roskilly, J. Chem. Phys. **100**, 1460 (1994).
[22] N. V. Madhusudana and G. Durand, J. Phys. (France) Lett. **46**, L195 (1985).
[23] J. P. Marcerou and J. Prost, Mol. Cryst. Liq. Cryst. **58**, 259 (1980).
[24] L. M. Blinov, M. Ozaki, and K. Yoshino, Pis'ma Zh. Eksp. Teor. Fiz. **69**, 220 (1999) [JETP Lett. **69**, 236 (1999)].
[25] T. Takahashi, S. Hasidate, H. Nishijou, M. Usui, M. Kimura, and T. Akahane, Jpn. J. Appl. Phys., Part 1 **37**, 1865 (1998).
[26] I. Dozov, I. Penchev, Ph. Martinot-Lagarde, and J. Durand, Ferroelectr. Lett. Sect. **2**, 135 (1984).
[27] B. Valenti, C. Bertoni, G. Barbero, P. Taverna-Valabrega, and R. Bartolino, Mol. Cryst. Liq. Cryst. **146**, 307 (1987).
[28] L. M. Blinov, M. Kozlovsky, K. Nakayama, M. Ozaki, and K. Yoshino, Jpn. J. Appl. Phys., Part 1 **35**, 5405 (1996).
[29] L. M. Blinov, M. Kozlovsky, T. Nagata, M. Ozaki, and K. Yoshino, Jpn. J. Appl. Phys., Part 2 **38**, L1042 (1999).
[30] D. S. Hermann, P. Rudquist, K. Ichimura, K. Kudo L. Komitov, and S. T. Lagerwall, Phys. Rev. E **55**, 2857 (1997).
[31] L. Komitov, C. Ruslim, and K. Ichimura, Phys. Rev. E **61**, 5379 (2000).
[32] C. J. F. Böttcher, *Theory of Electric Polarization* (Elsevier, Amsterdam, 1973).
[33] M. J. Frisch *et al.*, GAUSSIAN 98 (Gaussian Inc., Pittsburgh, PA, 1998).
[34] B. H. Besler, K. M. Merz, and P. A. Kollman, J. Comput. Chem. **11**, 431 (1990); U. C. Singh and P. A. Kollman, *ibid.* **5**, 129 (1984).
[35] M. F. Sanner, J.-C. Spenher, and A. J. Olson, Biopolymers **38**, 305 (1996).
[36] F. M. Richards, Annu. Rev. Biophys. Bioeng. **6**, 151 (1977); M. L. Connolly, J. Appl. Crystallogr. **16**, 548 (1983).
[37] A. Bondi, J. Phys. Chem. **68**, 441 (1964).
[38] G. Vertogen and W. H. de Jeu, *Thermotropic Liquid Crystals: Fundamentals* (Springer, Berlin, 1988).

[39] N. Kuze, H. Fujiwara, H. Takeuchi, T. Egawa, S. Konaka, and G. Fogarasi, J. Phys. Chem. A **103**, 3054 (1999).

[40] H. Hakemi, E. F. Jagodzinski, and D. B. Dupré, Mol. Cryst. Liq. Cryst. **91**, 129 (1983).

[41] N. Biswas and S. Umapathy, J. Phys. Chem. A **101**, 5555 (1997).

[42] G. G. Nair, S. K. Prasad, and C. V. Yelamaggad, J. Appl. Phys. **87**, 2084 (2000).